Molecular Catalysis 438 (2017) 113–120

Contents lists available at ScienceDirect

Molecular Catalysis

journal homepage: www.elsevier.com/locate/mcat

MCAT

Editor's choice paper

Kinetics and molecular mechanism of arsenite photochemical oxidation based on sulfate radical

Liyuan Chai[a,b], Jinqin Yang[a], Feng Liao[c], Qingzhu Li[a,b,*], Qingwei Wang[a,b], Hui Liu[a,b], Qiyu Dong[a], Zhipeng Yin[a]

[a] School of Metallurgy and Environment, Central South University, 932 South Lushan Road, Changsha, Hunan 410083, PR China
[b] Chinese National Engineering Research Center for Control & Treatment of Heavy Metal Pollution, 932 South Lushan Road, Changsha, Hunan, 410083, PR China
[c] School of Environmental Science and Engineering, Shanghai Jiao Tong University, 800 Dong Chuan Road, Shanghai 200240, PR China

ARTICLE INFO

Article history:
Received 15 January 2017
Received in revised form 7 March 2017
Accepted 12 March 2017

Keywords:
Arsenite
Oxidation
Sulfate radical
Kinetics
Molecular mechanism

ABSTRACT

Sulfate radical ($SO_4^{\bullet-}$) has great potential of becoming an alternative to hydroxyl radical ($HO^{\bullet}$) due to its strong oxidizing capability and adaptability in wastewater purification. In this study, the oxidation of arsenite (As(III)) based on $SO_4^{\bullet-}$ was conducted under xenon (Xe) lamp irradiation, where peroxydisulfate (PDS) was used as radical precursor. It was observed that the As(III) oxidation reaction was rapid and mainly proceeded in the initial few minutes. $SO_4^{\bullet-}$ was proved to be mainly responsible for the oxidation of As(III), but $HO^{\bullet}$ derived by $SO_4^{\bullet-}$ also made a contribution. Herein, the kinetics of the rapid As(III) oxidation was studied by the initial reaction rate method and results ($r_0 = k[As(III)]_0^{0.51}[PDS]_0^{0.64}$, where $k = 2.5 - 8.4 \times 10^{-2}\ M^{-0.15}\ s^{-1}$ and the apparent activation energy $E_a = 46.09\ kJ\ mol^{-1}$) indicate that As(III) oxidation is easily facilitated in PDS/Xe system. Finally, the molecular mechanism of As(III) oxidation by both $SO_4^{\bullet-}$ and its induced $HO^{\bullet}$ were investigated by density functional theory (DFT) methods The significant role of $SO_4^{\bullet-}$ on As(III) oxidation was therefore demonstrated both kinetically and mechanistically.

1. Introduction

Arsenic (As) contaminations have been paid decades' attention all over the world. Its over-standard concentration has been detected in ground and surface waters arising from the discharge of industrial waste containing As [1–3]. As prevalently exists as arsenite (As(III)) and arsenate (As(V)) in aquatic environment [4]. As(III) is predominant inorganic As species in smelting and mining effluents [5–7], and constitutes over 70% of dissolved As in groundwater samples [8]. Including precipitation [9,10], coagulation [11,12], ion exchange [13,14], adsorption [15–17] and so forth, many techniques are available for As removal but inclined to remove As(V). Consequently, pre-oxidation is an essential anchor for As(III)-contained water treatment.

Various methods (e.g., ozone [8], manganese and chlorine compounds [18,19], ferrate [20], and hydrogen peroxide [21]) have been studied for As(III) oxidation. In comparison, the catalyzed oxidation systems are more attractive due to rapid reaction, such as, Fenton ($Fe(II)/H_2O_2$) [22], Fenton-like ($Fe(III)/H_2O_2$) [23], photo-Fenton (UV/H_2O_2) [24] and TiO_2 photocatalytic system (UV/TiO_2) [25] etc. In these systems, the most important reactive species devoted to As(III) oxidation is determined as hydroxyl radical ($HO^{\bullet}$) and its reaction rate toward As(III) is very high ($8.5 \times 10^9\ M^{-1}\ s^{-1}$) under acidic conditions [26]. Similar to $HO^{\bullet}$, sulfate radical ($SO_4^{\bullet-}$) is also a strong oxidizing agent. It has been reported that $SO_4^{\bullet-}$ is more advantageous than $HO^{\bullet}$ due to a longer half-life and thus capable to escape from the solvent cage to oxidize As(III) [27,28]. Moreover, $SO_4^{\bullet-}$ is a very strong electron acceptor enabling reactions impossible for $HO^{\bullet}$ [22]. For example, perfluorinated carboxylic acids are inert towards $HO^{\bullet}$ but can be degraded by $SO_4^{\bullet-}$ [29,30].

A promising oxidation technique based on $SO_4^{\bullet-}$ has emerged over the past years to mineralize organic pollutants and oxidize As(III) [30–33]. The generation of $SO_4^{\bullet-}$ from peroxydisulfate (PDS, $S_2O_8^{2-}$) resembles that of $HO^{\bullet}$ from H_2O_2. The peroxide bond in radical precursors PDS and H_2O_2 can be broken by heat, ultraviolet, ultrasound, radiolysis, etc [33] to generate $SO_4^{\bullet-}$. Numerous activated methods (UV light [34], acoustic cavitation [31] and Fe(II) activation [35]) have thus been studied for As(III) oxidation by $SO_4^{\bullet-}$. For comparison with the $HO^{\bullet}$-based oxidation, As(III) oxidation based on $SO_4^{\bullet-}$ was discussed in this study under dark,

* Corresponding author at: School of Metallurgy and Environment, Central South University, 932 South Lushan Road, Changsha, Hunan, 410083, PR China.
E-mail addresses: chailiyuan@csu.edu.cn (L. Chai), jqin2014@icloud.com (J. Yang), qingzhuli@csu.edu.cn (Q. Li).

http://dx.doi.org/10.1016/j.mcat.2017.03.014
2468-8231/

daylight and the high intensive xenon (Xe) light conditions. Xe lamp, which can simulate solar light, is effective to activate PDS and then stimulate As(III) oxidation at room temperature [34]. In addition, we noticed that As(III) oxidation was rapid in the ferrous-activated PDS system, i.e., the initial few-minute reaction dominated in a 60-min oxidation process [35]. Curiously, is there a same trend of rapid As(III) oxidation in Xe-activated PDS system and how about its kinetics? Therefore, the kinetics of As(III) oxidation was emphatically investigated here in Xe-activated PDS system. As for oxidation mechanism, both $SO_4^{\bullet-}$ and $HO^{\bullet}$ were reported to play roles in As(III) oxidation *via* electron-transfer reaction [35]. Tetravalent As(IV) as an intermediate has been postulated in the metal (Fe(II), Fe(III) and Cu(II)) catalyzed As(III)-PDS systems [36–38]. In addition to the resultant $As(OH)_3^{\bullet+}$ of electron transfer reaction, $As(OH)_4^{\bullet}$, which is the product of $HO^{\bullet}$-based addition reaction, was also reported previously [39,40]. Unfortunately, there is no suitable detection method for various As intermediates and few studies on molecular mechanism of As(III) oxidation. Quantum chemical calculation is powerful to predict molecule structures, energies, spectral and reaction mechanisms. Accordingly, all possible reaction pathways were proposed and investigated in this study by DFT calculations performed with Gaussian 09 code. To the best of our knowledge, this is the first time to investigate the kinetics and molecular mechanism of As(III) oxidation in $SO_4^{\bullet-}$-based system.

2. Materials and methods

2.1. Materials and batch experiments

Chemically pure sodium arsenite ($NaAsO_2$) and sodium peroxydisulfate ($Na_2S_2O_8$, PDS) were purchased from Shanghai No.4 Chemical Reagent Factory (China) and Xilong Chemical Co., Ltd (China), respectively. Potassium borohydride (KBH_4), potassium hydroxide (KOH) and hydrochloric acid (HCl) were all guaranteed reagents and used for the determination of As(III) by hydride generation atomic fluorescence spectrometry (HG-AFS) method. Other chemicals were of analytical grade or better and used without further purification. Ultrapure water (Molro, Shanghai, China) was used throughout.

The As(III) stock solution was prepared weekly using $NaAsO_2$ and kept at 4 °C. PDS and H_2O_2 were respectively used for the daily preparation of PDS and H_2O_2 stock solutions. Aliquots of As(III) and PDS (or H_2O_2) stock solutions were combined to achieve the initial experimental conditions. Reactions were carried out in 250 ml beaker at 15 ± 1 °C water baths under exposure to air. The experiment apparatus and correlation parameters were shown in Fig. S1. Unless otherwise noted, xenon (Xe) lamp (CEL-HXUV300, Beijing CEAULIGTH) was used to commence the reaction and the initial pH was around 6. The emission spectrum of the Xe lamp is shown in Fig. S2. In the pH effect section, sulfuric acid was used for pH adjustment. The solutions were sampled periodically and mixed with excess methanol immediately for scavenging radicals and diluted with 5% HCl solution. The repeatability of experiments was illustrated in Fig. S3.

2.2. Analysis and calculation methods

The initial and residual As(III) concentrations were measured by an atomic fluorescence spectrophotometer (AFS-8230, Beijing Jitian Instruments Co., China). KBH_4 solution (2%, m/v) was prepared freshly by dissolving KBH_4 powder in KOH solution (0.5%, m/v). HCl solution (5%, v/v) was prepared from corresponding concentrated acid. To detect As(III) selectively, the working solutions include a mixture of 2% KBH_4 and 0.5% KOH as reducing solution and 5% HCl as carrier solution. Under these conditions, only As(III) was converted to AsH_3 and detected on an AFS instrument [41]. The calculation of oxidation yield was elaborated in another section below.

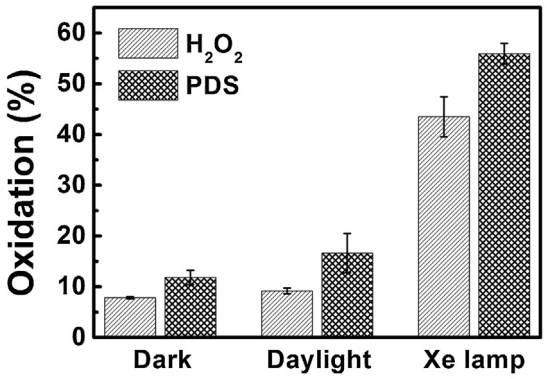

Fig. 1. The oxidation yield of As(III) by PDS or H_2O_2 after 30-min reaction under dark, daylight and Xe lamp. $[As(III)]_0 = 20\ \mu mol\ L^{-1}$, $[PDS]_0 = [H_2O_2]_0 = 10\ \mu mol\ L^{-1}$.

Electron spin resonance (ESR) experiments were conducted on a Bruker A200 ESR spectrometer within 2 min after starting the reaction. The experimental conditions were: center field 3500 G, sweep width 100 G, microwave frequency 9.81 GHz, microwave power 2.47 mW, modulation amplitude 0.5 G, conversion time 30 ms, time constant 164 ms, receiver gain 1×10^5 and number of scans 4. 5,5-dimethyl-1-pyrroline N-oxide (DMPO) was used as the spin trap for radical determination.

Quantum chemical calculations were carried out with Gaussian09 code. All geometrical structures were fully optimized at M06-2X/6-31G* level and vibrational frequency calculations were carried out at the same level to confirm the local minima character of the species and determine the zero-point vibrational energies and thermal corrections to the Gibbs free energies. The unrestricted open-shell approach was used for radical species. No spin contamination was found for radicals, i.e., the $<S^2>$ values were around 0.75. Single-point energies were calculated for the optimized geometries at M06-2X/6–311++G** level and the solvent (water) effect was modeled with the integral equation formalism version of the polarizable continuum model (IEFPCM). The free energy change ($\Delta G_{r,solv}$) of reactions corrected by thermal effects at 298 K were calculated as Eq. (1).

$$\Delta G_{r,solv} = \sum (E_0 + G_{corrected})_{product} - \sum (E_0 + G_{corrected})_{reactant} \quad (1)$$

3. Results and discussion

3.1. The $SO_4^{\bullet-}$-based As(III) oxidation

To compare the As(III) oxidation based on $SO_4^{\bullet-}$ and $HO^{\bullet}$, commonly used oxidants PDS and H_2O_2 were chosen to oxidize As(III) under dark, daylight and xenon (Xe) lamp conditions. The molar ratio of oxidant to As(III) was maintained at 0.5 ($R_{ox/As(III)} = 0.5$) in this part. As shown in Fig. 1, the oxidation yields in PDS system were all higher than in H_2O_2 system. Thus, PDS is advantageous over H_2O_2 for As(III) oxidation, especially under Xe lamp irradiation. It was also reported that PDS was more effective than H_2O_2 for oxidizing monomethylarsonic acid (MMA) and dimethylarsinic acid (DMA) under UV irradiation [42]. In particular, the oxidation yield is 56% in PDS/Xe combination, whereas only 12% and 17% in PDS/dark and PDS/daylight combination, respectively. Therefore, PDS/Xe is an effective combination for As(III) oxidation, where $SO_4^{\bullet-}$ may be generated due to the decomposition of PDS under Xe lamp irradiation [34]. Here, Xe lamp solar simulator can emit the light of continuous band from UVA to visible range (Fig. S2).